Biochemical and Biophysical Research Communications 391 (2010) 1131–1135

Contents lists available at ScienceDirect

Biochemical and Biophysical Research Communications

journal homepage: www.elsevier.com/locate/ybbrc

Structural insights into the substrate recognition properties of β-glucosidase

Ki Hyun Nam, Min Woo Sung, Kwang Yeon Hwang *

Division of Biotechnology, College of Life Sciences & Biotechnology, Korea University, Seoul 136-701, South Korea

ARTICLE INFO

Article history:
Received 4 December 2009
Available online 11 December 2009

Keywords:
β-Glucosidase
Catalysis processing
Intermediate state
Substrate specificity
Steric hindrance

ABSTRACT

β-Glucosidase enzymes (EC 3.2.1–3.2.3) hydrolyze sugars and are implicated in a wide spectrum of biological processes. Recently, we reported that β-glucosidase has varied kinetic parameters for the natural and synthetic substrates [K.H Nam, S.J. Kim, M.Y. Kim, J.H. Kim, T.S. Yeo, C.M. Lee, H.K Jun, K.Y. Hwang. Crystal structure of engineered beta-glucosidase from a soil metagenome, Proteins 73 (2008) 788-793]. However, an understanding of the kinetic values of β-glucosidase has not yet enabled the elucidation of its molecular function. Here, we report the X-ray crystal structure of β-glucosidase with a glucose and cellobiose fragment from uncultured soil metagenome. From the various crystals, we obtained the pre-reaction (native), intermediate (disaccharide cleavage) and post-reaction (glucose binding) states of the active site pocket. These structures provide snapshots of the catalytic processing of β-glucosidase. In addition, the intermediate state of the crystal structure provides insight into the substrate specificity of β-glucosidase. These structural studies will facilitate elucidation of the architectural mechanism responsible for the substrate recognition of β-glucosidase.

© 2009 Elsevier Inc. All rights reserved.

Introduction

The astronomical number of possible combinations for a small oligosaccharide results in a structural and functional diversity for these compounds that is far greater than that possible for peptides or nucleic acids of comparable size [1]. Oligo- and polysaccharides thus play central roles in a diverse array of biological processes, which include structural roles, the storage and utilization of food, viral invasion, and highly selective cellular signaling events. β-Glucosidase enzymes (EC 3.2.1–3.2.3) hydrolyze these sugars (i.e., glycoside hydrolases) and are implicated in a wide spectrum of biological processes. In general, β-glucosidase enzymes cleave the β-1,4-glucosidic bonds in a variety of glucosides [2]. Two carboxylic acids are involved in catalysis at the active site. One residue functions as the catalytic nucleophile by attacking at the substrate anomeric centre to form a covalent α-D-glucosyl enzyme intermediate, while the other carboxyl group acts as an acid/base catalyst by protonating the glycosidic oxygen in the first step and deprotonating the nucleophilic water molecule in the second step. Considerable evidence exists in support of these mechanisms [3–6].

Defects in the genes encoding glycoside hydrolases are responsible for many genetically inherited diseases including lysosomal storage disorders, and for this reason, specific inhibitors of glycoside hydrolysis offer potential as therapeutic agents [2,7]. In addition, heritable deficiencies in glycosyl hydrolases are common genetic diseases e.g., lactose intolerance and the large group of lysosomal storage diseases [8]. Various β-glucosidase structures were determined, and these aided in understanding the function of this enzyme; however, structural studies of β-glucosidase have focused on inhibitors and analogue substrates. Therefore, a structural understanding of the substrate-specific activation of β-glucosidase is not sufficient to elucidate its properties fully. Recently we reported the crystal structure and biological characterization of β-glucosidase from metagenome library. This protein has varied kinetic parameters fors pNP-β-glucoside, cellobiose and sophorose, which are 33.6, 0.376 and 2.58 Kcat/km (mM/s), respectively [9].

Here, we report the X-ray crystal structures of β-glucosidase complexed with a glucose and cellobiose fragment from uncultured soil metagenome. From the various crystals, we obtained the pre-reaction (native), intermediate (disaccharide cleavage) and post-reaction (glucose binding) states of the active site pocket. These structures provide snapshots of the catalytic processing of β-glucosidase. In addition, the intermediate state of the crystal structure provides insight into the substrate specificity of β-glucosidase. The information presented here will contributes to the overall understanding of substrate recognition.

Materials and methods

Protein production, activity assessment and crystallization. The cloning, purification and crystallization of β-glucosidase from a

* Corresponding author. Fax: +82 2 923 3229.
E-mail address: chahong@korea.ac.kr (K.Y. Hwang).

0006-291X/$ - see front matter © 2009 Elsevier Inc. All rights reserved.
doi:10.1016/j.bbrc.2009.12.038

metagenome library has previously been reported [9]. Briefly, the gene for hexahistidine-tagged β-glucosidase was cloned into the pET28a vector, and expressed in *Escherichia coli* BL21(DE3). The protein was purified using a two-step purification protocol consisting of affinity and size-exclusion chromatography. The purified protein was concentrated to 20 mg/ml in 50 mM Tris–HCl pH 7.0 prior to crystallization. The crystals were grown from a well solution containing 0.1 M Tris–HCl, pH 7.0–7.4 and 0.8 M Na/K tartrate equilibrated at 22 °C against 0.5 ml of precipitation solution using the hanging-drop vapor-diffusion method.

Substrate soaking and data collection. The protein crystal was soaked into the same crystallization drop volume of 50% glucose and 25 mM cellobiose (which was dissolved in the reservoir solution). It was then dehydrated in air for a period of ~5 min. The data sets were collected using a synchrotron radiation source using beamlines 4A and 6C of the Pohang Light Source (PLS, South Korea). The data were indexed and scaled using the software HKL2000 [10]. Data collection statistics are reported in Table 1.

Structure solution and refinement. The structure of β-glucosidase from the metagenome library was determined using the molecular replacement method, using the coordinates of β-glucosidase–tartaric acid structure from the metagenome library (PDB code 3CMJ) as a search model [9]. Crystallographic refinement was performed using the CNS program [11]. Several rounds of energy minimization refinement were alternated with rebuilding using the Coot program [12]. At the last stage, water, metal and substrate molecules were included and were combined with additional rounds of positional and individually-restrained B-factor refinements. The final refinement structure statistics are reported in Table 1. The geometry of the final model was checked using PROCHECK [13] and the figures were generated using PyMOL [14]. Buried vertices were calculated using the PDBsum program [15].

Accession code. Atomic coordinates and structure factors were deposited in the Protein Data Bank under the accession codes 3FIY (pre-reaction state), 3FJ0 (intermediate state) and 3FIZ (post-reaction state).

Results

Data collection and structure determination

The initial crystallization conditions included tartaric acid (PDB code 3CMJ), and at this stage, tartaric acid interacted with the active site of β-glucosidase. This tartaric acid molecule can be displaced by a high affinity substrate [16], and therefore these crystallization conditions can be used to obtain the structure of the substrate complex. A displacement strategy has been proposed for the crystallographic analysis of glycosidases, which exploits the potential use of sugars as cryoprotectants [17,18]. Therefore, we soaked the protein crystals in 50% glucose and 25 mM disaccharide (i.e., cellobiose, gentiobiose or sophorose) and incubated them for ~30 min. We did not use the cryoprotectant solution when collecting diffraction data. We determined the pre-reaction (gentiobiose and sophorose), intermediate-(cellobiose) and post-reaction (glucose) states of the catalytic site of β-glucosidase from the various data sets.

Overall structure and active site pocket

A detailed description of the structural characteristics of engineered β-glucosidase obtained from the metagenome library has been reported previously [9]. Here, we describe the crystal structure of β-glucosidase complexed either with glucose or cellobiose fragment, and the uncomplexed form. The three crystal structures of β-glucosidase have a rigid TIM barrel fold (Fig. 1A). The r.m.s. deviations range between 0.05 and 0.1 Å for 498 Cα atom pairs (Lys42–Glu481) when the structures are compared. Specifically, four loops (L1, L2, L3 and L4) on the TIM barrel fold of β-glucoside have different conformation for substrate binding [19]. In our crys-

Table 1
Data collection and refinement statistics.

	Pre-reaction	Intermediate	Post-reaction
Data collection			
Space group	$P2_12_12_1$	$P2_12_12_1$	$P2_12_12_1$
Cell parameters			
a, b, c (Å)	70.43, 71.16, 87.25	70.30, 71.14, 87.01	70.38, 70.56, 86.58
Resolution (Å)	20–1.4	20–1.15	20–2.0
Measured reflections	339750	763135	115846
Unique reflections	82773	141384	28542
Completeness	95.2 (88.9)	91.3 (61.1)	95.8 (89.1)
Redundancy	4.1 (2.9)	5.4 (3.1)	4.1 (2.9)
I/σ (I)	28.5 (2.57)	29.2 (2.02)	12.3 (2.14)
R_{merge} (%)	4.3 (24.9)	4.8 (31.9)	8.1 (26.6)
Refinement			
Resolution (Å)	19.99–1.4	20–1.15	19.95–2.0
R_{work}/R_{free} (%)	18.5/20.1	21.0/21.6	17.9/21.3
R.m.s deviations			
Bond lengths (Å)	0.006	0.008	0.007
Bond angles (°)	1.3	1.4	1.4
Ramachandran plot (%)			
Most favored	90.4	90.4	90.4
Additionally allowed	8.8	8.8	8.6
Generously allowed	0.8	0.8	1.0

The highest resolution shell is shown in parentheses.
[a] $R_{merge} = \sum h \sum i|I(h,ii) - <I(h)>|/\sum h \sum iI(h,ii)$, where $I(h,i)$ is the intensity of the ith measurement of reflection h and $<I(h)$ is the mean value of $I(h,i)$ for all i measurements.
[b] $R_{work} = \sum||F_{obs}| - |F_{calc}||/\sum|F_{obs}|$, where F_{obs} and F_{calc} are the observed and calculated structure-factor amplitudes, respectively. R_{free} was calculated as R_{work} using a randomly selected subset (10%) of unique reflections not used for structure refinement.
[c] Categories were defined using PROCHECK.

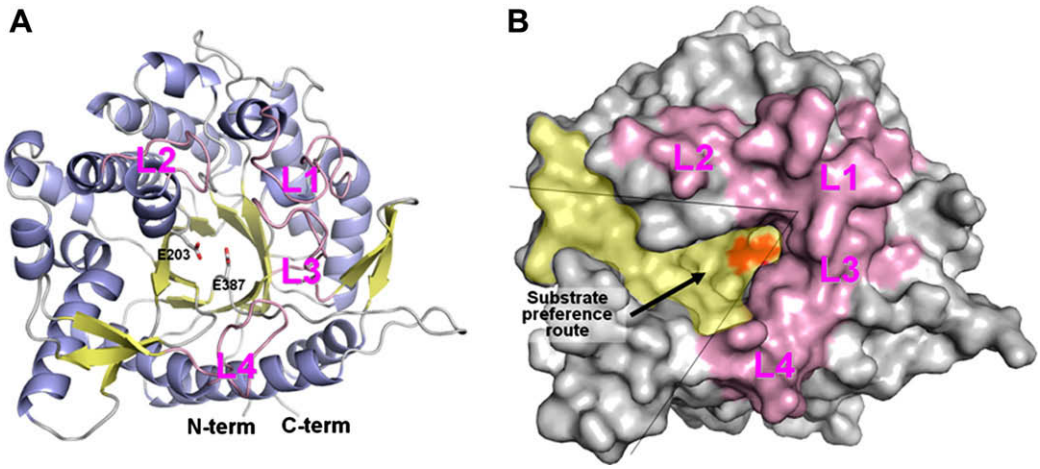

Fig. 1. Crystal structure of β-glucosidase. (A) Overall structure of β-glucosidase. Catalytic residues are represented using a stick model. The four loops where the substrate enters are colored in pink. (B) Representation of the surface structure. The large cleft is colored in yellow. The four loops where the substrate enters are colored in pink. Based on an analysis of the structure, the substrate prefers the route from the cavity of the rigid structure (see the detailed description in the text).

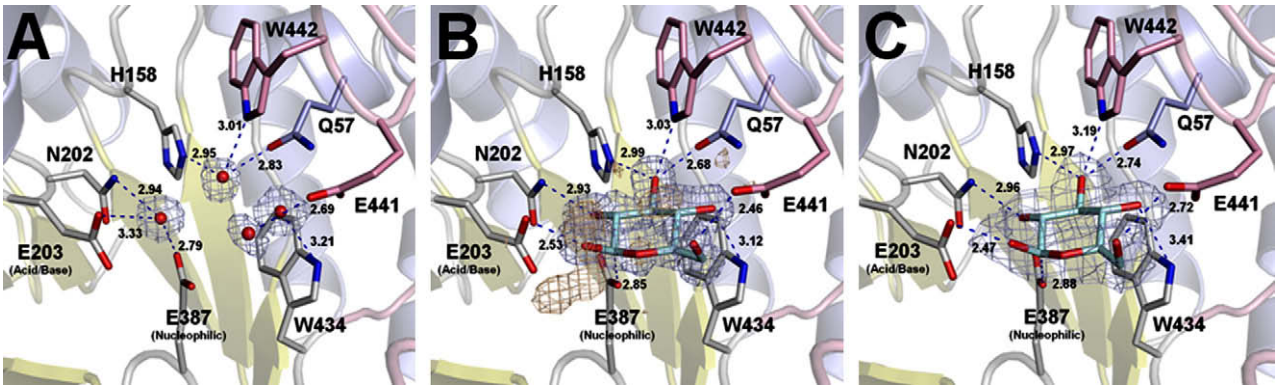

Fig. 2. Complex structures of active site pocket in β-glucosidase. Snapshots of the catalytic process of β-glucosidase in the (A) pre-reaction state, the (B) intermediate state, and the (C) post-reaction state. The electron density of each substrate is shown and was obtained using the final sigma A-weighted 2Fo–Fc electron density map contoured at 1σ (cyan). In the transition state, the electron density map (beige color) is indicated in the Fo–Fc electron density map contoured at 3σ. The polar interactions between the enzyme and the substrate are indicated by broken lines.

tal structure, however, these loops regions are also similar to other complexes. The structure of the active site pocket without any substrate, on the TIM barrel fold, has approximate dimensions of 5 × 5 × 10 Å, and forms a partial negative surface. β-Glucosidase has a large cleft in the active site pocket, with accessible vertices of 70.15, buried vertices of 12.41 and an average depth of 16.24 Å. This cleft had a cavity of approximately 15 × 10 Å; therefore the related disaccharides substrate could easily enter the active site pocket, based on this structural analysis. We therefore, conclude that substrates approach preferentially from the cavity (Fig. 1B).

Complex structures of active site pocket in β-glucosidase

In the pre-reaction state of β-glucosidase (Fig. 2A), the active site pocket remained empty in the absence of tartaric acid, i.e., we observe that the occupancy of water is higher than that of tartaric acid. Tartaric acid was present in the soaking conditions of gentiobiose and sophorose. While these disaccharides were not observed in the active site pocket, four water molecules were clearly present at this site. The water molecules were coordinated by the following active site residues: the Oε atom of Glu203 (acid–base), the Oε atom of Glu387 (nucleophilic), the Oε atom of Gln57, the Nε atom of His158, the Nδ atom of Asn202, the Nε atom of Trp434, the Oε atom of Glu441, and the Nε atom of Trp442. The coordinated atom interactions were within 3.33, 2.79, 2.83, 2.95, 2.94, 3.21, 2.69 and 3.01 Å, respectively, of three water molecules. When compared with other structures, these three water molecules are at positions similar to those of the hydroxyl group of the glucose moiety.

In the intermediate state of β-glucosidase (Fig. 2B), β-D-glucoside was easily detected in the S1 pocket, which is the pocket before the cleavage position, using an electron density map. However, the second β-D-glucoside position (termed S1′ pocket, which is adjacent to the cleavage position) is absent from the electron density map, indicating that it was loosely bound in the pocket, or that its occupancy was low. The glycosidic bond position is observed, however. The β-D-glucoside molecules in the S1 pocket were coordinated with the following active site residues: the Oε atom of Glu203 (acid–base), the Oε atom of Glu387 (nucleophilic), the Oε atom of Gln57, the Nε atom of His158, the Nδ atom of Asn202, the Nε atom of Trp434, the Oε atom of Glu441, and the Nε atom of Trp442. The coordinated atom interactions were within 2.53, 2.85, 2.68, 2.99, 2.93, 3.12, 2.46 and 3.03 Å, respectively, of the first β-D-glucoside. This structure tightly interacted with the active site, more so than the water molecules. Specifically, we

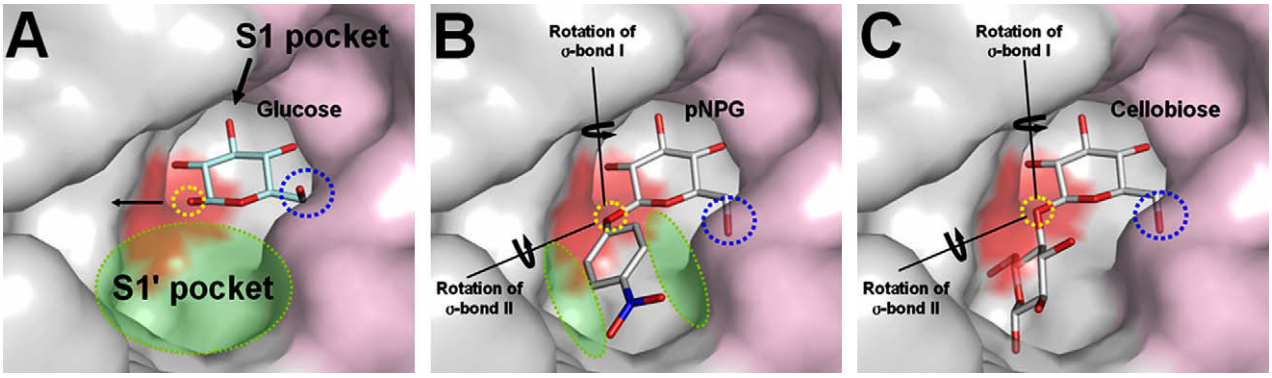

Fig. 3. Proposal of a substrate specificity (enzyme kinetics) model of β-glucosidase based on steric hindrance. (A) In the intermediate structure, β-D-glucose was stabilized and fixed in place by neighboring residues on the S1 pocket. (B) In the model structure with pNPG bound, the glucose of pNPG has a similar binding mode and its nitrophenyl group is relatively free to move about in the S1′ pocket. (C) In the energy minimized cellobiose-binding model structure, the S1 pocket is filled by the first glucose of cellobiose; however, the second glucose of cellobiose in the S1′ pocket overlaps with the surface of the active site pocket. This second glucose of cellobiose will change the conformation of the substrate and will be used in the rotation of the σ-bond of the glucoside (see the detailed description in the text); thus the substrate configuration will affect the enzyme kinetics. The hydroxyl group in this model (B, C), shown in a blue-dotted circle, will change the conformation of the molecule. The cleavage site is indicated by the yellow-dotted circle.

observed that Glu203 (acid–base) shared the electron density map with the β-D-glucoside of cellobiose in the S1 pocket; we consider that this intermediate state form is bound covalently. Although we did not determine the atomic position of the β-D-glucoside of cellobiose in the S1′ pocket clearly, this structure provides information on the substrate specificity, based on the Fo–Fc electron density map (discussed below).

In the post-reaction state of β-glucosidase (Fig. 2C), glucose was easily detected in an electron density map. The β-D-glucoside molecules were coordinated with the following active site residues: the Oε atom of Glu203 (acid–base), the Oε atom of Glu387 (nucleophilic), the Oε atom of Gln57, the Nε atom of His158, the Nδ atom of Asn202, the Nε atom of Trp434, the Oε atom of Glu441, and the Nε atom of Trp442. The coordinated atom interactions were within 2.47, 2.88, 2.74, 2.97, 2.96, 3.41, 2.72 and 3.19 Å, respectively, of the β-D-glucoside. The interactions in this structure were similar to those of the intermediate state; we consider this structure to be the final catalysis step (disaccharide cleavage) of β-glucosidase. Structural analysis of the three structures present in the active site pocket revealed that the binding mode of the first glucose of the cellobiose fragment, in particular the atomic position of the hydroxyl group, is very similar to the binding mode found in the glucose-complexed structure. Superimposing the interaction of these residues revealed r.m.s. deviations ranging between 0.05 and 0.1 Å for Glu203 (acid–base), Glu387 (nucleophilic), Gln57, His158, Asn202, Trp434, Glu441 and Trp442. Therefore the active site of β-glucosidase contains a rigid formation, which is independent of the substrate and stabilized by hydroxyl groups, either from the substrate or from water.

Discussion

In this report, we propose a model for the substrate preference and specificity of β-glucosidase by using the intermediate and model structures. Based on structural analysis, we found that the second glucose position has a low occupancy. We observe that the second glucose interacts weakly, or not at all, with its neighboring residues in the active site pocket, because the β-D-glucose in the S1′ pocket has to dissociate easily during catalysis. Structural analysis shows that neighboring residues in the active site pocket form a structure that is too rigid, which makes the pocket fixed. This means that the kinetics of β-glucosidase will depend on the configuration of the substrate. In the intermediate structure, β-D-glucose binds to the S1 pocket, and this structure is stabilized and fixed into position by the neighboring residues. The bond to be cleaved by glucosidase is close to the active site residues (Fig. 3A). In the pNPG model structure, the pNPG glucose has a similar binding mode and its nitrophenyl group is located in the S1′ pocket. In this model, the bond to be cleaved was close to the active site residues and the small-sized nitrophenyl group was relatively free to move in the S1′ pocket (Fig. 3B). In the energy minimized cellobiose model structure, cellobiose also shared the glucose binding mode in the S1 pocket (Fig. 3C); however, the second glucose of cellobiose overlapped with the surface of the S1′ pocket. Our experiments showed that β-glucosidase has a strongly rigid structure in the S1 substrate binding site. Thus the second glucose of cellobiose will change the conformation of the substrate using the rotation of the σ-bond of the glucoside. Therefore, cellobiose has a lower Kcat/km than the substrate pNPG, as cellobiose requires a conformational change for catalysis.

In summary, we have determined the pre-reaction, intermediate and post-reaction states of β-glucosidase with analogue and natural substrates. These structures provide snapshots of the catalytic processing of β-glucosidase. Specifically, the intermediate state of the crystal structure provides insights into the substrate specificity of β-glucosidase. Based on these results, we suggest that the glucose in the S1′ pocket may determine the kinetic activity of the enzyme using steric hindrance, thus affecting substrate specificity during catalysis. We believe that these results will contribute to understanding of the kinetics of β-glucosidase.

Acknowledgments

We thank Dr. H.S. Lee, K.J. Kim, and K.H. Kim for their kind assistance with the data collection using beamlines 4A and 6C of the Pohang Light Source, Korea. This study was supported by the Korea Science and Engineering Foundation. [R01-2007-000-20072-0 (2009)]. K.H. Nam is supported by the BK21 program.

References

[1] B. Henrissat, G. Davies, Structural and sequence-based classification of glycoside hydrolases, Curr. Opin. Struct. Biol. 7 (1997) 637–644.
[2] G. Taylor, Sialidases: structures, biological significance and therapeutic potential, Curr. Opin. Struct. Biol. 6 (1996) 830–837.
[3] C.S. Rye, S.G. Withers, Glycosidase mechanisms, Curr. Opin. Chem. Biol. 4 (2000) 573–580.
[4] H.D. Ly, S.G. Withers, Mutagenesis of glycosidases, Annu. Rev. Biochem. 68 (1999) 487–522.
[5] M.W. Bauer, R.M. Kelly, The family 1 beta-glucosidases from *Pyrococcus furiosus* and *Agrobacterium faecalis* share a common catalytic mechanism, Biochemistry 37 (1998) 17170–17178.

[6] J. Chir, S. Withers, C.F. Wan, Y.K. Li, Identification of the two essential groups in the family 3 beta-glucosidase from *Flavobacterium meningosepticum* by labeling and tandem mass spectrometric analysis, Biochem. J. 365 (2002) 857–863.
[7] M. von Itzstein, P. Colman, Design and synthesis of carbohydrate-based inhibitors of protein–carbohydrate interactions, Curr. Opin. Struct. Biol. 6 (1996) 703–709.
[8] B. Henrissat, I. Callebaut, S. Fabrega, P. Lehn, J.P. Mornon, G. Davies, Conserved catalytic machinery and the prediction of a common fold for several families of glycosyl hydrolases, Proc. Natl. Acad. Sci. USA 92 (1995) 7090–7094.
[9] K.H. Nam, S.J. Kim, M.Y. Kim, J.H. Kim, Y.S. Yeo, C.M. Lee, H.K. Jun, K.Y. Hwang, Crystal structure of engineered beta-glucosidase from a soil metagenome, Proteins 73 (2008) 788–793.
[10] Z. Otwinowski, W. Minor, Processing of X-ray diffraction data collected in oscillation mode, Methods Enzymol. 276 (1997) 307–326.
[11] A.T. Brunger, P.D. Adams, G.M. Clore, W.L. DeLano, P. Gros, R.W. Grosse-Kunstleve, J.S. Jiang, J. Kuszewski, M. Nilges, N.S. Pannu, R.J. Read, L.M. Rice, T. Simonson, G.L. Warren, Crystallography & NMR system: a new software suite for macromolecular structure determination, Acta Crystallogr. D Biol. Crystallogr. 54 (1998) 905–921.
[12] P. Emsley, K. Cowtan, Coot: model-building tools for molecular graphics, Acta Crystallogr. D Biol. Crystallogr. 60 (2004) 2126–2132.
[13] P.A. Laskowski, M.W. McArthur, D.S. Moss, J.M. Thornton, PROCHECK: a program to check the stereochemical quality of protein structures, J. Appl. Cryst. 26 (1993) 283–291.
[14] W.L. DeLano, The PyMOL molecular graphics system. Available from: <http://www.pymol.org>.
[15] R.A. Laskowski, PDBsum: summaries and analyses of PDB structures, Nucleic Acids Res. 29 (2001) 221–222.
[16] B.W. Sigurskjold, Exact analysis of competition ligand binding by displacement isothermal titration calorimetry, Anal. Biochem. 277 (2000) 260–266.
[17] E.F. Garman, T.R. Schneider, Macromolecular cryocrystallography, J. Appl. Crystallog. 30 (1997) 211–237.
[18] P. Isorna, J. Polaina, L. Latorre-García, F.J. Cañada, B. González, J. Sanz-Aparicio, Crystal structures of *Paenibacillus polymyxa* beta-glucosidase B complexes reveal the molecular basis of substrate specificity and give new insights into the catalytic machinery of family I glycosidases, J. Mol. Biol. 371 (2007) 1204–1218.
[19] M. Czjzek, M. Cicek, V. Zamboni, D.R. Bevan, B. Henrissat, A. Esen, The mechanism of substrate (aglycone) specificity in beta-glucosidases is revealed by crystal structures of mutant maize beta-glucosidase-DIMBOA, -DIMBOAGlc, and -dhurrin complexes, Proc. Natl. Acad. Sci. USA 97 (2000) 13555–13560.